Article

NMR Structure of the Complex between the Tfb1 Subunit of TFIIH and the Activation Domain of VP16: Structural Similarities between VP16 and p53

Chantal Langlois, Caroline Mas, Paola Di Lello, Lisa M. Miller Jenkins, Pascale Legault, and James G. Omichinski

J. Am. Chem. Soc., **2008**, 130 (32), 10596-10604 • DOI: 10.1021/ja800975h • Publication Date (Web): 17 July 2008

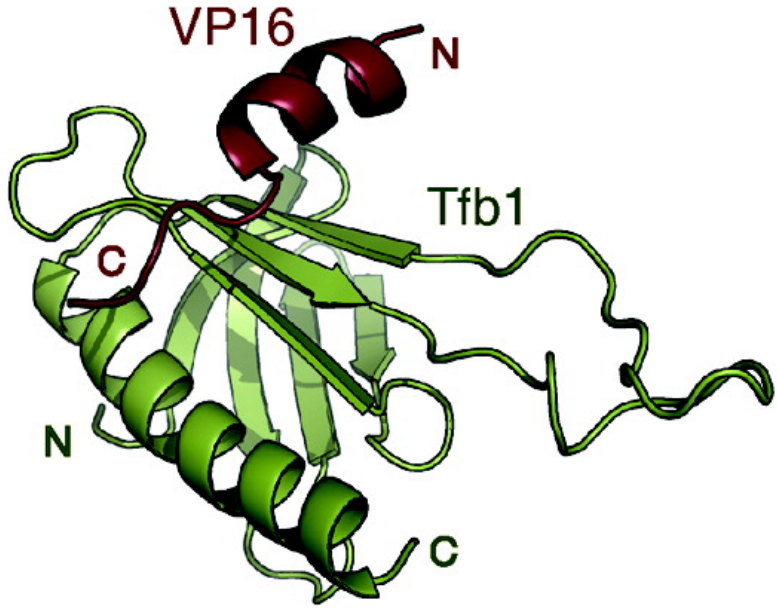

More About This Article

Additional resources and features associated with this article are available within the HTML version:

- Supporting Information
- Access to high resolution figures
- Links to articles and content related to this article
- Copyright permission to reproduce figures and/or text from this article

View the Full Text HTML

J|A|C|S
ARTICLES

Published on Web 07/17/2008

NMR Structure of the Complex between the Tfb1 Subunit of TFIIH and the Activation Domain of VP16: Structural Similarities between VP16 and p53

Chantal Langlois,[†] Caroline Mas,[†] Paola Di Lello,[†] Lisa M. Miller Jenkins,[‡] Pascale Legault,[†] and James G. Omichinski*,[†]

Département de Biochimie, Université de Montréal, C.P. 6128 Succursale Centre-Ville, Montréal, QC H3C 3J7 Canada, and Laboratory of Cell Biology, NCI, National Institutes of Health, 37 Convent Drive, Bethesda, Maryland 20892-4256

Received February 7, 2008; E-mail: jg.omichinski@umontreal.ca

Abstract: The Herpes Simplex Virion Protein 16 (VP16) activates transcription through a series of protein/protein interactions involving its highly acidic transactivation domain (TAD). The acidic TAD of VP16 (VP16TAD) has been shown to interact with several partner proteins both *in vitro* and *in vivo*, and many of these VP16 partners also bind the acidic TAD of the mammalian tumor suppressor protein p53. For example, the TADs of VP16 and p53 (p53TAD) both interact directly with the p62/Tfb1 (human/yeast) subunit of TFIIH, and this interaction correlates with their ability to activate both the initiation and elongation phase of transcription. In this manuscript, we use NMR spectroscopy, isothermal titration calorimetery (ITC) and site-directed mutagenesis studies to characterize the interaction between the VP16TAD and Tfb1. We identify a region within the carboxyl-terminal subdomain of the VP16TAD (VP16C) that has sequence similarity with p53TAD2 and binds Tfb1 with nanomolar affinity. We determine an NMR structure of a Tfb1/VP16C complex, which represents the first high-resolution structure of the VP16TAD in complex with a target protein. The structure demonstrates that like p53TAD2, VP16C forms a 9-residue α-helix in complex with Tfb1. Comparison of the VP16/Tfb1and p53/Tfb1 structures clearly demonstrates how the viral activator VP16C and p53TAD2 shares numerous aspects of binding to Tfb1. Despite the similarities, important differences are observed between the p53TAD2/Tfb1 and VP16C/Tfb1 complexes, and these differences demonstrate how selected activators such as p53 depend on phosphorylation events to selectively regulate transcription.

Introduction

Activators function by stimulating transcription through protein/protein interactions involving their transactivation domain (TAD).[1,2] The current model is that activators function by recruiting a number of different transcriptional regulatory factors including nucleosome-remodeling complexes, the mediator complex and several general transcription factors (TFIIB, TBP, TFIIH) to enhance the rate of transcription by affecting nucleosome assembly/disassembly, preinitiation complex formation, promoter clearance and/or the rate of elongation.[3–17] Originally, transcription activators were classified based on the presence of specific amino acids within their TAD, and these included the acidic-rich (aspartic and glutamic acid), the glutamine-rich, the proline-rich and the serine/threonine-rich activators.[2] Given their occurrence in a number of crucial transcriptional regulatory proteins, the most extensively studied activators are those that contain acidic TADs and two highly investigated acidic activators are the human tumor suppressor protein p53 and the Herpes Simplex Virion (HSV) protein 16 (VP16).[18,19]

VP16 functions to stimulate transcription of viral immediate early genes in HSV-infected cells, whereas p53 induces the

[†] Université de Montréal.
[‡] National Institutes of Health.

(1) Ptashne, M.; Gann, A. A. F. *Nature* **1997**, *386*, 569–577.
(2) Ptashne, M.; Gann, A. A. F. *Nature* **1990**, *346*, 329–331.
(3) Prochasson, P.; Neely, K. E.; Hassan, A. H.; Li, B.; Workman, J. L. *Mol. Cell* **2003**, *12* (4), 983–990.
(4) Gutierrez, J. L.; Chandy, M.; Carrozza, M. J.; Workman, J. L. *EMBO J.* **2007**, *26* (3), 730–740.
(5) Bryant, G. O.; Ptashne, M. *Mol. Cell* **2003**, *11*, 1301–1309.
(6) Goodrich, J. A.; Hoey, T.; Thut, C. J.; Admon, A.; Tjian, R. *Cell* **1993**, *75*, 519–530.
(7) Brown, S. A.; Weirich, C. S.; Newton, E. M.; Kingston, R. E. *EMBO J.* **1998**, *17*, 3146–3154.
(8) Blau, J.; Xiao, H.; McCracken, S.; O'Hare, P.; Greenblatt, J.; Bentley, D. *Mol. Cell. Biol.* **1996**, *16*, 2044–2055.
(9) Bentley, D. *Curr. Opin. Genet. Dev.* **1995**, *5*, 210–216.
(10) Brown, C. E.; Howe, L.; Sousa, K.; Alley, S. C.; Carrozza, M. J.; Tan, S.; Workman, J. L. *Science* **2001**, *292* (5525), 2333–2337.
(11) Ito, M.; Yuan, C.-X.; Malik, S.; Gu, W.; Fondell, J. D.; Yamamura, S.; Fu, Z.-Y.; Zhang, X.; Qin, J.; Roeder, R. G. *Mol. Cell* **1999**, *3* (3), 361–370.
(12) Black, J. C.; Choi, J. E.; Lombardo, S. R.; Carey, M. *Mol. Cell* **2006**, *23* (6), 809–818.
(13) Hall, D. B.; Struhl, K. *J. Biol. Chem.* **2002**, *277*, 46043–46050.
(14) Kuras, L.; Struhl, K. *Nature* **1999**, *399* (6736), 609–613.
(15) Yang, F.; et al. *Nature* **2006**, *442* (7103), 700–704.
(16) Yang, F.; DeBeaumont, R.; Zhou, S.; Naar, A. M. *Proc. Natl. Acad. Sci. U.S.A.* **2004**, *101* (8), 2339–2344.
(17) Tansey, W. P.; Ruppert, S.; Tjian, R.; Herr, W. *Genes Dev.* **1994**, *8* (22), 2756–2769.
(18) Fields, S.; Jang, S. K. *Science* **1990**, *249* (4972), 1046–1049.
(19) Triezenberg, S. J.; Kingsbury, R. C.; McKnight, S. L. *Genes Dev.* **1988**, *2*, 718–729.

 10.1021/ja800975h CCC: $40.75

expression of many human target genes whose products regulate numerous functions, including cell-growth arrest and apoptosis.[20,21] The acidic TADs of VP16 (residues 412−490) and p53 (residues 1−72) share many similarities related to both their functions and amino acid composition.[18–20,22,23] The TAD of both VP16 and p53 can be divided into two subdomains, and each subdomain is capable of independently activating transcription when tethered to a DNA-binding domain. In the case of VP16, the subdomains are referred to as the amino subdomain (VP16N or $VP16_{412-456}$) and the carboxyl subdomain (VP16C or $VP16_{456-490}$),[6,22,24–26] whereas for p53 they are referred to as the first TAD (p53TAD1 or $p53_{1-40}$) and the second TAD (p53TAD2 or $p53_{40-72}$).[27] Mutagenesis studies have clearly demonstrated that the activity of VP16 and p53 depends not only on acidic residues but also on key hydrophobic and aromatic amino acids within their respective TADs.[22,26,28–33] Importantly, both the p53 and the VP16 TADs have been shown to interact directly with several of the same target proteins both *in vitro* and *in vivo*, and these targets include the TATA-binding protein (TBP), the CREB-binding protein (CBP), the general transcription factor IIB (TFIIB), TBP-associated factor (TAF) $TAF_{II}31$ and the p62/Tfb1 (human/yeast) subunit of the general transcription factor IIH (TFIIH).[6,13,17,34–39]

Given the high percentage of aspartic acid and glutamic acid residues within their sequences, acidic TADs are generally thought to be devoid of regular secondary structure elements in their free state and have been referred to as "acid blobs" or "negative noodles".[40] NMR studies of the TADs of p53 and VP16 in their free state support this view.[41–43] In some cases, it has been shown that acidic TADs become more ordered when bound to their target proteins[31,33,44–49] and that the intrinsically unstructured nature of TADs helps them mediate multiple protein/protein interactions with different partners.[50] Three high-resolution structures have been determined for complexes containing one of the two subdomains of the p53TAD: a p53TAD1/MDM2 complex,[45] a p53TAD2/RPA70 (replication protein A 70) complex[47] and a p53TAD2/Tfb1 (Tfb1 subunit of TFIIH) complex.[49] In all three complexes, the TAD of p53 adopts a short α-helical conformation in the presence of its partner protein.

Despite the fact that the VP16TAD has been extensively studied and utilized as a model activation domain to examine activation mechanisms and protein interactions in a wide number of organisms including mammals,[51] yeast[52] and plants,[53] there is currently no high-resolution structure of a protein/protein complex containing the VP16TAD. Previous NMR studies have examined the structure of the TAD of VP16 in complex with the $TAF_{II}31$,[31] the human cofactor protein PC4 and TFIIB.[33] In the first study, VP16C ($VP16_{456-490}$) complexed to $TAF_{II}31$ was predicted to form an α-helix between residues 472 and 483.[31] In the second study, the full-length TAD of VP16 ($VP16_{412-490}$) in complex with either PC4 or TFIIB forms two α-helices.[33] The first helix was between residues 435 and 450 within VP16N and the second helix was between residues 465 and 485 in VP16C. In this study, models of VP16N and VP16C in complex with either PC4 or TFIIB were proposed based on docking approaches in combination with NMR chemical shift mapping. In both studies, high-resolution structures of the complexes were not obtained.[31,33] Therefore, the current mechanism by which the VP16TAD recognizes its target partners at the atomic level is poorly understood.

It has previously been demonstrated that the TADs of VP16 and p53 directly bind the p62/Tfb1 subunit of TFIIH and that their binding to TFIIH correlates directly with their ability to activate both the initiation and elongation phase of transcription.[8,54] In this manuscript, we have used Isothermal Titration Calorimetry (ITC), NMR spectroscopy and site-directed mutagenesis experiments to define the molecular basis of the interaction between the TAD of VP16 and the Tfb1 subunit of TFIIH. We demonstrated by ITC that VP16C binds to Tfb1 with higher affinity then VP16N. We determined by NMR spectroscopy a high-resolution structure of a complex between Tfb1 and

(20) Levine, A. J. *Cell* **1997**, *88*, 323–331.
(21) Wysocka, J.; Herr, W. *Trends Biochem. Sci.* **2003**, *28* (6), 294–304.
(22) Cress, W. D.; Triezenberg, S. J. *Science* **1991**, *251*, 87–90.
(23) Das, G.; Hinkley, C. S.; Herr, W. *Nature (London)* **1995**, *374* (6523), 657–660.
(24) Sullivan, S. M.; Horn, P. J.; Olson, V. A.; Koop, A. H.; Niu, W.; Ebright, R. H.; Triezenberg, S. J. *Nucleic Acid Res.* **1998**, *26*, 4487–4496.
(25) Mitchell, P. J.; Tjian, R. *Science* **1989**, *245*, 371–378.
(26) Regier, J. L.; Shen, F.; Triezenberg, S. J. *Proc. Natl. Acad. Sci. U.S.A.* **1993**, *90*, 883–887.
(27) Candau, R.; Scolnick, D. M.; Darpino, P.; Ying, C. Y.; Halazonetis, T. D.; Berger, S. L. *Oncogene* **1997**, *12*, 807–816.
(28) Hope, I. A.; Mahadevan, S.; Struhl, K. *Nature* **1988**, *333*, 635–640.
(29) Gill, G.; Sadowski, I.; Ptashne, M. *Proc. Natl. Acad. Sci. U.S.A.* **1990**, *87*, 2127–2131.
(30) Drysdale, C. M.; Duenas, E.; Jackson, B. M.; Reusser, U.; Braus, G. H.; Hinnebusch, A. G. *Mol. Cell. Biol.* **1995**, *15*, 1230–1233.
(31) Uesugi, M.; Nyanguile, O.; Lu, H.; Levine, A. J.; Verdine, G. L. *Science* **1997**, *277*, 1310–1313.
(32) Uesugi, M.; Verdine, G. L. *Proc. Natl. Acad. Sci. U.S.A.* **1999**, *96* (26), 14801–14806.
(33) Jonker, H. R. A.; Wechselberger, R. W.; Boelens, R.; Folkers, G. E.; Kaptein, R. *Biochemistry* **2005**, *44* (3), 827–839.
(34) Stringer, K. F.; Ingles, C. J.; Greenblatt, J. *Nature* **1990**, *345*, 783–786.
(35) Ingles, C. J.; Shales, M.; Cress, W. D.; Triezenberg, S. J.; Greenblatt, J. *Nature* **1991**, *351*, 588–590.
(36) Neeley, K. E.; Hassan, A. H.; Wallberg, A. E.; Steger, D. J.; Cairns, B. R.; Wrights, A. P.; Workman, J. L. *Mol. Cell* **1999**, *4*, 649–655.
(37) Neeley, K. E.; Hassan, A. H.; Brown, C. E.; Howe, L.; Workman, J. L. *Mol. Cell. Biol.* **2002**, *22*, 1615–1625.
(38) Yudkovsky, N.; Logie, C.; Hanh, S.; Peterson, C. L. *Genes Dev.* **1999**, *13*, 2369–2374.
(39) Chang, J.; Kim, D.-H.; Lee, S. W.; Choi, K. Y.; Sung, Y. *J. Biol. Chem.* **1995**, *270* (42), 25014–25019.
(40) Sigler, P. B. *Nature* **1988**, *333*, 210–212.
(41) O'Hare, P.; Williams, G. *Biochemistry* **1992**, *31*, 4150–4156.
(42) Lee, H.; Mok, K. H.; Muhandiram, R.; Park, K.-Y.; Suk, J.-E.; Kim, D.-H.; Chang, J.; Sun, Y. C.; Choi, K. Y.; Han, K.-H. *J. Biol. Chem.* **2000**, *275*, 29426–29432.
(43) Donaldson, L.; Capone, J. P. *J. Biol. Chem.* **1992**, *267*, 1411–1414.
(44) Shen, F.; Triezenberg, S. J.; Hensley, P.; Porter, D.; Knutson, J. R. *J. Biol. Chem.* **1996**, *271*, 4827–4837.
(45) Kussie, P. H.; Gorina, S.; Marechal, V.; Elenbaas, B.; Moreau, J.; Levine, A. J.; Pavletich, N. P. *Science* **1996**, *274*, 948–953.
(46) Lee, C.; Chang, J. H.; Lee, H. S.; Cho, Y. *Genes Dev.* **2002**, *16*, 3199–3212.
(47) Bochkareva, E.; Kaustov, L.; Ayed, A.; Yi, G.-S.; Lu, Y.; Pineda-Lucena, A.; Liao, J. C. C.; Okorokov, A. L.; Milner, J.; Arrowsmith, C. H.; Bochkarev, A. *Proc. Natl. Acad. Sci. U.S.A.* **2005**, *102* (43), 15412–15417.
(48) Chi, S.-W.; Lee, S.-H.; Kim, D.-H.; Ahn, M.-J.; Kim, J.-S.; Woo, J.-Y.; Torizawa, T.; Kainosho, M.; Han, K.-H. *J. Biol. Chem.* **2005**, *280* (46), 38795–38802.
(49) Di Lello, P.; Jenkins, L. M. M.; Jones, T. N.; Nguyen, B. D.; Hara, T.; Yamaguchi, H.; Dikeakos, J. D.; Appella, E.; Legault, P.; Omichinski, J. G. *Mol. Cell* **2006**, *22* (6), 731–740.
(50) Dyson, H. J.; Wright, P. E. *Curr. Opin. Struct. Biol.* **2002**, *12* (1), 54–60.
(51) Uhlmann, T.; Boeing, S.; Lehmbacher, M.; Meisterernst, M. *J. Biol. Chem.* **2007**, *282* (4), 2163–2173.
(52) Taddei, A.; Van Houwe, G.; Hediger, F.; Kalck, V.; Cubizolles, F.; Schober, H.; Gasser, S. M. *Nature* **2006**, *441* (7094), 774–778.
(53) Moore, I.; Samalova, M.; Kurup, S. *Plant J.* **2006**, *45* (4), 651–683.
(54) Xiao, H.; Pearson, A.; Coulombe, B.; Truant, R.; Zhang, S.; Regier, J. L.; Trienzenberg, S. J.; Reinberg, D.; Flores, O.; Ingles, C. J.; Greenblatt, J. *Mol. Cell. Biol.* **1994**, *14*, 7013–7024.

VP16C. This structure demonstrates that like p53, VP16C forms a 9-residue α-helix when bound to Tfb1 and that several residues within the α-helix make important hydrophobic, cation-π and ionic interactions with Tfb1. Structural comparison of the Tfb1/VP16 complex with our previously published Tfb1/p53 complex[49] indicates that the two complexes are strikingly similar. The two structures explain how the TAD of VP16 can mimic mammalian activators such as p53. In addition, there are important differences between the Tfb1/p53 and Tfb1/VP16 complexes that help explain how activation domains can selectively regulate transcription, and these differences appear to be related to the phosphorylation state of p53. Such detailed structural information is absolutely essential to our efforts to design molecules that mimic transcription activators such as p53 and VP16.

Experimental Procedures

Cloning of Recombinant Proteins. $Tfb1_{1-115}$ and related mutants were constructed as GST-fusion proteins as previously described.[49] Dr. Steven Triezenberg generously provided the clones expressing $VP16_{412-456}$ (VP16N) and $VP16_{456-490}$ (VP16C) as GST-fusion proteins. Site directed mutagenesis of VP16C and addition of a tyrosine residue at the carboxyl-terminal position of the VP16N segment were carried out with the QuickChange II site-directed mutagenesis kit (Stratagene).

Protein Expression and Purification. $Tfb1_{1-115}$ and its mutant were purified as previously described.[49,55] VP16N, VP16C and VP16C mutants were expressed as GST-fusion protein in *Escherichia coli* host strain TOPP2 and bound to GSH-resin (General Electric). The resin bound protein was incubated overnight with thrombin (Calbiochem). Following cleavage, the supernatant was purified using a Q-Sepharose High Performance column (General Electric). Uniformly (>98%) ^{15}N-labeled and $^{15}N/^{13}C$-labeled proteins were prepared in minimal media containing $^{15}NH_4Cl$ and/or $^{13}C_6$-glucose as the sole nitrogen and carbon sources.[55]

Isothermal Titration Calorimetry Studies. The ITC titration experiments were performed as previously described[56] in 20 mM TRIS at pH 7.5. The concentrations of the injected proteins were determined from A_{280}. All titrations fit the single-binding site mechanism with 1:1 stoichiometry.

NMR Samples. For the NMR structural studies of the $Tfb1_{1-115}$/VP16C complex, we used four samples. One sample contained 1.0 mM of ^{15}N-$Tfb1_{1-115}$ in 10 mM sodium phosphate (pH 6.5), 1 mM EDTA and 90% H_2O/10% D_2O; unlabeled VP16C was added to a final ratio of 1:1. The second sample consisted of 1.0 mM of $^{15}N/^{13}C$-$Tfb1_{1-115}$ in 10 mM sodium phosphate (pH 6.5), 1 mM EDTA and 90% H_2O/10% D_2O to which unlabeled VP16C was added to a final ratio of 1:1. The third sample contained 1.0 mM of ^{15}N-VP16C in 10 mM sodium phosphate (pH 6.5), 1 mM EDTA and 90% H_2O/10% D_2O; unlabeled $Tfb1_{1-115}$ was added to a final ratio of 1:1. The fourth sample consisted of 1.0 mM of $^{15}N/^{13}C$-VP16C in 10 mM sodium phosphate (pH 6.5), 1 mM EDTA and 90% H_2O/10% D_2O to which unlabeled $Tfb1_{1-115}$ was added to a final ratio of 1:1. For experiments in D_2O, samples two and four were lyophilized and resuspended in 100% D_2O.

For the NMR mapping studies of the $Tfb1_{1-115}$/VP16C complex, we used two samples. One sample contained 0.5 mM of ^{15}N-$Tfb1_{1-115}$ in 10 mM sodium phosphate (pH 6.5), 1 mM EDTA and 90% H_2O/10% D_2O; unlabeled VP16C was added to a final ratio of 1:1. The second sample consisted of 0.5 mM of ^{15}N- VP16C in 10 mM sodium phosphate (pH 6.5), 1 mM EDTA and 90% H_2O/10% D_2O to which unlabeled $Tfb1_{1-115}$ was added to a final ratio of 1:1.

NMR Spectroscopy. The NMR experiments were carried out at 300 K on Varian Unity Inova 500 and 600 MHz spectrometers. The backbone and aliphatic side chain resonances (^1H, ^{15}N and ^{13}C) were assigned using a combination of triple resonance experiments [HNCO, HNCACB, (HB)CBCA(CO)NNH, C(CO)NNH, H(CCO)NNH and HCCH-COSY]. Interproton distance restraints were derived from ^{15}N-edited NOESY-HSQC and ^{13}C-edited HMQC-NOESY spectra ($\tau_m = 90$ ms). The NMR data were processed with NMRPipe/NMRDraw[57] and analyzed with NMRView.[58]

Structure Calculations. The NOE-derived distance restraints were divided into three classes defined as strong (1.8−2.8 Å), medium (1.8−3.4 Å) and weak (1.8−5.0 Å). Backbone dihedral angles were derived with the program TALOS.[59] Following exchange in D_2O, slow-exchanging amide protons were identified by recording a 2D $^1H-^{15}N$ HSQC spectrum of $Tfb1_{1-115}$. Hydrogen bonds were used as distance restraints only for the slowly exchanging amide protons in elements of secondary structure and after the initial rounds of calculations had revealed the protein fold. The structures of VP16C and the PH domain of $Tfb1_{1-115}$ were calculated using the program CNS, with a combination of torsion angle and Cartesian dynamics[60] and starting from two extended structures with standard geometry. The quality of the structures was assessed using PROCHECK-NMR[61] and MOLMOL.[62] All of the figures representing the structures were generated with the program PyMol (http://www.pymol.org).

Results

VP16C Binds the PH Domain of Tfb1 with Higher Affinity than VP16N. We have previously shown by chemical shift mapping studies that VP16N binds to the amino-terminal PH domain of Tfb1 ($Tfb1_{1-115}$) and that the binding site for VP16N on Tfb1 is virtually identical to the binding site for p53TAD2 on Tfb1.[49,55] Since both VP16N and VP16C are each capable of independently activating transcription and VP16C has been shown to interact with a number of transcriptional regulatory proteins including TBP, PC4,TFIIB, TAF9 and $TAF_{II}31$,[24,31,33,63] we investigated whether or not VP16C was also able to interact with Tfb1. To check this, we determined the dissociation constants (K_d) for the complexes formed between VP16N and $Tfb1_{1-115}$ and between VP16C and $Tfb1_{1-115}$ by ITC (Supplementary Figure 1, Supporting Information). By this method, VP16C bound to Tfb1 with an apparent K_d of 360 ± 40 nM and VP16N bound to Tfb1 with an apparent K_d of 1000 ± 100 nM (Table 1). These results suggested that both subdomains of the VP16TAD were capable of interacting with Tfb1, and the K_d obtained for the Tfb1/VP16C complex is very similar to the K_d observed between Tfb1 and the p53TAD2 (390 nM).[49] Our VP16C binding to Tfb1 (360 nM), as measured by ITC, is higher affinity than what has been previously reported for VP16C

(55) Di Lello, P.; Nguyen, B. D.; Jones, T. N.; Potempa, K.; Kobor, M. S.; Legault, P.; Omichinski, J. G. *Biochemistry* **2005**, *44* (21), 7678–7686.
(56) Houtman, J. C. D.; Higashimoto, Y.; Dimasi, N.; Cho, S.; Yamaguchi, H.; Bowden, B.; Regan, C.; Malchiodi, E. L.; Mariuzza, R.; Schuck, P.; Appella, E.; Samelson, L. E. *Biochemistry* **2004**, *43* (14), 4170–4178.
(57) Delaglio, F.; Grzesiek, S.; Vuister, G. W.; Zhu, G.; Pfeifer, J.; Bax, A. *J. Biomol. NMR* **1995**, *6* (3), 277–293.
(58) Johnson, B. A.; Blevins, R. A. *J. Biomol. NMR* **1994**, *4*, 603–614.
(59) Cornilescu, G.; Delaglio, F.; Bax, A. *J. Biomol. NMR* **1999**, *13*, 289–302.
(60) Brunger, A. T.; Adams, P. D.; Clore, G. M.; Gros, P.; Grosse-Kunstleve, R. W.; Jiang, J.-S.; Kuszewski, J.; Nilges, M.; Pannu, N. S.; Read, R. J.; Rice, L. M.; Simonson, T.; Warren, G. L. *Acta Crystallogr.* **1998**, *D54*, 905–921.
(61) Laskowski, R. A.; Antoon, J.; Rullmann, C.; Macarthur, M. W.; Kaptein, R.; Thornton, J. M. *J. Biomol. NMR* **1996**, *8* (4), 477–486.
(62) Koradi, R.; Billeter, M.; Wüthrich, K. *J. Mol. Graphics* **1996**, *14*, 51–55.
(63) Nedialkov, Y. A.; Triezenberg, S. J. *Arch. Biochem. Biophys.* **2004**, *425* (1), 77–86.

Table 1. Comparison of the K_d (nM) Values for the Binding of VP16 and $Tfb1_{1-115}$ Using ITC

$Tfb1_{1-115}$	VP16N	1000 ± 100
$Tfb1_{1-115}$	VP16C	360 ± 40
$Tfb1_{1-115}$	VP16C (D472A)	2000 ± 300
$Tfb1_{1-115}$	VP16C (F475P)	NB[a]
$Tfb1_{1-115}$	VP16C (F475A)	1000 ± 200
$Tfb1_{1-115}$	VP16C (F479P)	NB
$Tfb1_{1-115}$	VP16C (F479A)	900 ± 100
$Tfb1_{1-115}$	VP16C (M478P)	NB[a]
$Tfb1_{1-115}$ (Q49A)	VP16C	NB[a]
$Tfb1_{1-115}$ (K11E)	VP16C	250 ± 30

[a] NB, no binding detected $K_d \geq 100$ μM.

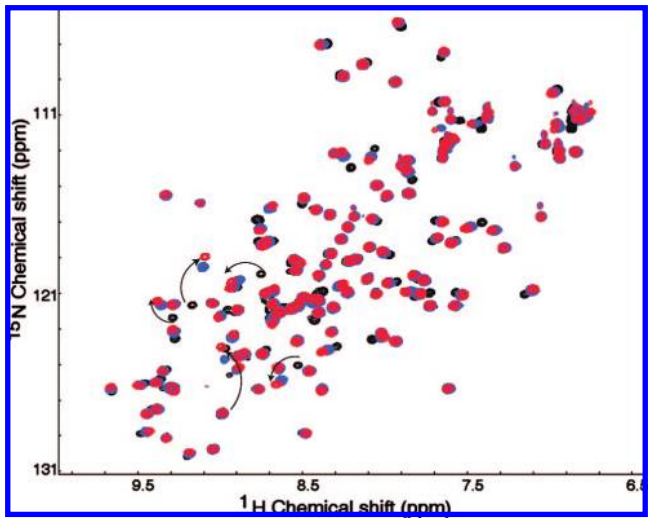

Figure 1. VP16C binds to the PH domain of Tfb1. Overlay of the 2D $^{1}H-^{15}N$ HSQC spectra for ^{15}N-labeled $Tfb1_{1-115}$ in its free form (black), in the presence of 0.75 equivalent (blue) and 1 equivalent (red) of VP16C.

binding to TFIIB (3 μM), PC4 (14 μM), TAF9 (73 μM) and human$TAF_{II}31$ (100 μM) but lower affinity then VP16C binding to yeast TBP (44 nM).[31,33,63]

VP16C Binds to the Same Region of the PH Domain of Tfb1 as VP16N. To define the binding site for VP16C on Tfb1, NMR chemical shift mapping studies were performed. Addition of VP16C ($VP16_{456-490}$) to ^{15}N-labeled $Tfb1_{1-115}$ produced changes in ^{1}H and ^{15}N chemical shifts for several signals of $Tfb1_{1-115}$ in the 2D $^{1}H-^{15}N$ HSQC spectra (Figure 1). The residues displaying significant chemical-shift changes ($\Delta\delta >$ 0.1 ppm; $\Delta\delta = [(0.17\Delta N_H)^2 + (\Delta H_N)^2]^{1/2}$) are clustered on a positively charged surface that includes strands β5, β6 and β7 of the PH domain when mapped onto the NMR solution structures of free Tfb1 (Supplementary Figure 2, Supporting Information). The VP16C binding site on Tfb1 is virtually identical to the binding sites for VP16N.[55] This result indicates that VP16C and VP16N share a common binding site on Tfb1 and this binding site is virtually identical to the binding site for p53TAD2.

Structure Determination of the Tfb1/VP16C Complex. Given the similar affinity of VP16C for $Tfb1_{1-115}$ and that VP16C shares a common binding site on Tfb1 with p53TAD2, we pursued NMR structural studies of a complex containing $Tfb1_{1-115}$ and VP16C. The NMR structure of a Tfb1/VP16C complex would not only provides us with the first high-resolution structure of the TAD of VP16 bound to a target protein, but it would allows us to make direct structural comparison between the TADs of p53 and VP16 bound to an identical target (Tfb1 in this case).[49]

Table 2. Structural Statistics of the Tfb1/VP16C Complex[a]

Restraints used for the structure calculations	
Total number of NOE distances restraints	1568
Short-range (intraresidue)	578
Medium-range ($\|i-j\| \leq 4$)	640
Long-range	309
Intermolecular	41
Hydrogen bond	36
Number of dihedral angle restraints (φ, ψ)	158
Structural statistics	
Rms deviations from idealized geometry	
Bonds (Å)	0.0025 ± 0.00006
Angles (deg)	0.3918 ± 0.0057
Impropers (deg)	0.2753 ± 0.132
Rms deviations from distance restraints (Å)	0.0215 ± 0.0005
Rms deviations from dihedral restraints (deg)	0.4438 ± 0.0357
Ramachandran statistics (%)[b]	
Residues in most favored regions	82.7
Residues in additional allowed regions	15.8
Residues in generously allowed regions	1.4
Residues in disallowed regions	0.2
Coordinate precision	
Atomic pairwise rmsd (Å)[c]	
Tfb1/VP16C complex	
Backbone atoms (C′, C^{α}, N)	0.74 ± 0.16
All heavy atoms	1.42 ± 0.19
Tfb1 alone	
Backbone atoms (C′, C^{α}, N)	0.62 ± 0.12
All heavy atoms	1.31 ± 0.17
VP16C alone	
Backbone atoms (C′, C^{α}, N)	0.43 ± 0.23
All heavy atoms	1.57 ± 0.37

[a] The 20 conformers with the lowest energy were selected for statistical analysis. Due to the absence of medium-range, long-range, and intermolecular NOEs involving residues 456−468 and 483−490 of VP16C, these amino acids were not included in the structure calculations. [b] Based on PROCHECK-NMR analysis. [c] Only residues 4−64 and 85−112 of Tfb1 and residues 470−482 of VP16C were used for rmsd calculations. Residues at the N-terminus (1−3), at the C-terminal (113−115) and in the flexible loop (65−84) of Tfb1, as well as residues at the N-terminus (456−468) and at the C-terminus (484−490) of VP16C, were not included in the calculation.

The three-dimensional structure of the $Tfb1_{1-115}$/VP16C complex was calculated using 1568 NOE-derived distance restraints, 36 hydrogen-bond restraints and 158 dihedral angle restraints. A total of 109 structures were calculated, and 100 of them satisfied the experimental constraints with no NOE violation greater than 0.2 Å and no backbone dihedral angle violation greater than 2° (Table 2). The structure of the $Tfb1_{1-115}$/VP16C complex is well defined by the NMR data (Figure 2). The 20 lowest-energy structures are characterized by good backbone geometry, no significant restraint violation and low pairwise rmsd values (Figure 2A and Table 2).

Structure of Tfb1 and VP16C in the Tfb1/VP16C Complex. The structure of Tfb1 in the Tfb1/VP16 complex is very similar to what was seen for the free form[55] and for the Tfb1/p53 complex.[49] Tfb1 contains a PH fold, which consists of two perpendicular antiparallel β-sheets arranged in a β-sandwich and flanked on one side by a long α-helix (Figure 2). This indicates that Tfb1 does not undergo any significant structural change between the free and the VP16C-bound forms.

The free VP16C is very flexible in solution and it does not appear to possess any regular elements of secondary structure.[31,33,41,43] Binding of VP16C to targets such as $TAF_{II}31$, TFIIB and PC4 induces formation of an α-helical structure

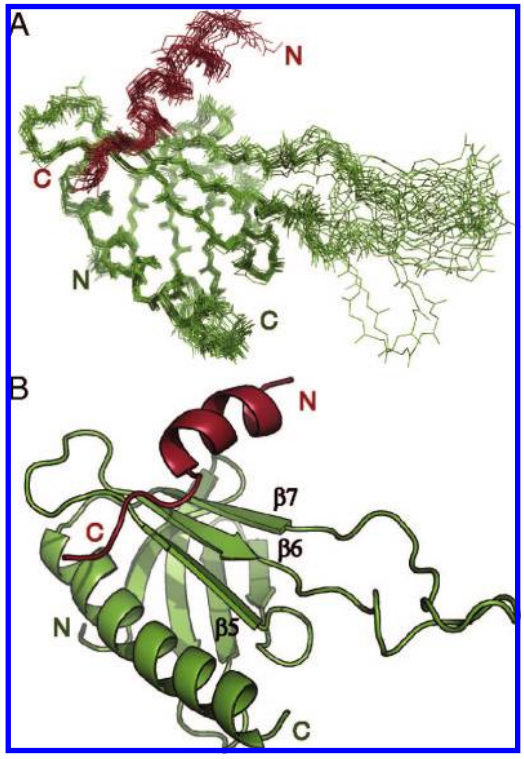

Figure 2. Structure of the Tfb1/VP16C complex. (A) Overlay of the 20 lowest-energy structures of the complex between $Tfb1_{1-115}$ (green) and VP16C (red). The structures were superimposed using the backbone atoms C′, C^{α} and N of residues 4−65 and 85−112 of Tfb1 and residues 470−482 of VP16C. (B) Ribbon representation of the lowest-energy structure of the $Tfb1_{1-115}$ /VP16C complex.

within VP16C.[31,33] In the case of $TAF_{II}31$, the α helix is located between residues 472 and 483, whereas with TFIIB and PC4 the α-helix is located between residues 465 and 485.[31,33] These helices were inferred from NMR studies based on NOE intensities. In the Tfb1/VP16C complex, chemical shift mapping studies demonstrate that addition of unlabeled Tfb1 to ^{15}N-labeled VP16C induced changes in the ^{1}H and ^{15}N chemical shifts of several signals in the 2D ^{1}H−^{15}N HSQC spectra of VP16C (Supplementary Figure 3, Supporting Information). As was observed for p53 in complex with Tfb1,[49] VP16C forms a short 9-residue α-helix between residues 472 and 480 (Figure 2B). Except for this 9-residue helix and a few flanking amino acids, VP16C is largely unstructured in complex with Tfb1.

Important Interactions at the Interface of the Tfb1/VP16C Complex. The binding interface of the Tfb1/VP16C complex comprises strands β5, β6 and β7 and the loop connecting β5 and β6 of Tfb1 and the 9-residue α-helix of VP16C (Asp^{472}−Thr^{480}). The VP16C helix is amphipathic and its hydrophobic face interacts with Tfb1. Three hydrophobic residues (Phe^{475}, Met^{478} and Phe^{479}) within the VP16C helix contribute a series of crucial contacts with Tfb1(Figure 3A). The aromatic side chain of Phe^{475} and Phe^{479} fill two adjacent shallow pockets on the surface of Tfb1, where they form a complex network of interactions with Gln^{49}, Met^{59}, Arg^{61} and Met^{88} of Tfb1 (Figure 3). The aromatic ring of Phe^{475} is positioned to form a cation-π interaction with Arg^{61} and a sulfur-π interaction with Met^{88} on

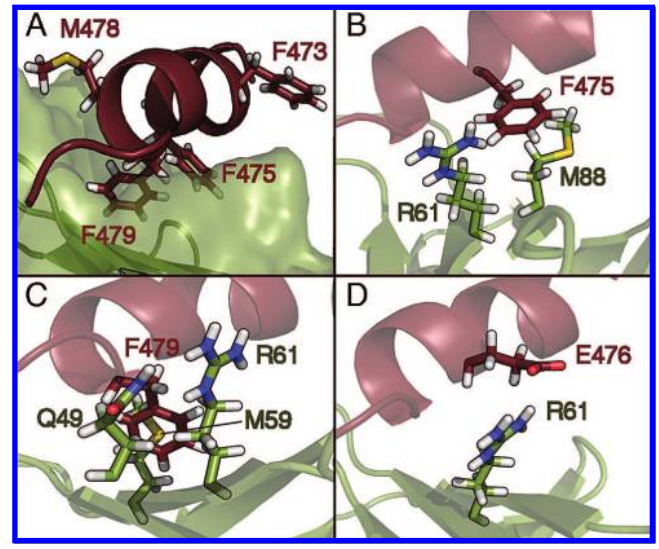

Figure 3. Structural details of the $Tfb1_{1-115}$/VP16C interface. (A) 3D structure of Tfb1 is shown as a ribbon within the transparent molecular surface (green), and the helix of VP16C is represented as a ribbon (red). (B−D) Backbone of Tfb1 and VP16C are shown as ribbons (green and red, respectively). (B) Phe^{475} of VP16C forms cation-π and sulfur-π interactions with Arg^{61} and Met^{88} of Tfb1, respectively. (C) Phe^{479} of VP16C forms cation-π, amino-aromatic and sulfur-π interactions with Arg^{61}, Gln^{49} and Met^{58} of Tfb1, respectively. (D) Arg^{61} of Tfb1 forms an ionic interaction with Glu^{476} of VP16C.

Tfb1 (Figure 3B).[64,65] In a similar manner to what was seen with Phe^{54} of p53 in the p53/Tfb1 complex, Phe^{479} of VP16C binds in a pocket formed by Gln^{49}, Ala^{50}, Thr^{51}, Met^{59}, Leu^{60} and Arg^{61} of Tfb1 (Figure 3B−C). In this pocket, the aromatic ring of Phe^{479} is positioned to participate in an amino-aromatic interaction with Gln^{49}, a sulfur-π interaction with Met^{59} and a cation-π interaction with Arg^{61} of Tfb1 (Figure 3C).[64–66] The third important hydrophobic residue in VP16C is Met^{478}. Met^{478} is inserted in a narrow cleft on the surface of Tfb1 formed by Lys^{57} and Met^{59}, where it makes van der Waals contacts with the side chains of Lys^{57} and Met^{59} of Tfb1. Like the p53 binding site,[49] the VP16C binding site on Tfb1 is characterized by a positively charged surface formed by Lys^{47}, Arg^{61}, and Arg^{86} that helps to position the negatively charged VP16C. In addition, one specific ionic interaction is observed involving Glu^{476} of VP16C and Arg^{61} of Tfb1 ($d_{N\zeta-O\varepsilon2} = 2.1$ Å in the minimized average structure) (Figure 3D).

ITC and Mutational Studies of the Interaction between VP16C and Tfb1. In earlier studies, we demonstrated via ITC and mutational analysis that Gln^{49} on Tfb1 makes key contributions to the binding of Tfb1 to p53.[49] In our Tfb1/VP16C structure, Gln^{49} is positioned to make crucial interactions with Phe^{479} of VP16C, and it is a key member of a complex interaction network on the surface of Tfb1. Therefore, we were interested in determining if mutation of Gln^{49} to alanine [Tfb1(Q49A)] would significantly alter the binding of Tfb1 to VP16C, as was observed for Tfb1 binding to p53TAD2. This mutant was selected because it is positioned on the surface of Tfb1 and we have previously demonstrated that this mutation does not significantly alter the structure of the PH domain of Tfb1.[49] ITC experiments of VP16C with Tfb1(Q49A) demonstrated that Gln^{49} is important for the formation of the Tfb1/VP16C complex as we were unable to detect binding for this

(64) Gallivan, J. P.; Dougherty, D. A. *Proc. Natl. Acad. Sci. U.S.A.* **1999**, *96* (17), 9459–9464.
(65) Reid, K. S. C.; Lindley, P. F.; Thornton, J. M. *FEBS Lett.* **1985**, *190* (2), 209–213.
(66) Burley, S. K.; Petsko, G. A. *FEBS Let.* **1986**, *203*, 139–143.

mutant (Table 1). This dramatic effect of the Q49A mutation on the binding of Tfb1 to VP16C is identical to what was observed with the Tfb1/p53 complex.

To assess the contribution of residues in the VP16C helix to Tfb1 binding, we performed site-directed mutagenesis at the three hydrophobic positions that make important contributions to the Tfb1/VP16C interface and we examined the binding of Tfb1 to the VP16C mutants by ITC (Table 1). In this assay, we were unable to detect binding to the VP16C(F475P), VP16C(M478P) and VP16C(F479P) mutants and these results indicate that these three VP16C mutants have K_d'$s \geq 100\ \mu$M (Table 1). This is consistent with the fact that proline would significantly impair formation of the helix in VP16C. Replacing either Phe[475] or Phe[479] by alanine had a less dramatic effect.[24,63] As measured by the ITC method, VP16C(F475A) bound to Tfb1 with an apparent K_d of 1000 ± 200 nM and VP16C (F479A) bound to Tfb1 with an apparent K_d of 900 ± 100 nM (Table 1). These results are in agreement with our structural studies indicating that these three hydrophobic residues are important for formation of the interface between Tfb1 and VP16. In addition, these results are consistent with the fact that VP16C(F475P) and VP16C(F479P) are almost completely devoid of transcriptional activation activity whereas VP16C(F475A) and VP16C(F479A) retain approximately 20−25% of their transcriptional activity.[63]

Previously, we have shown that binding of p53TAD2 to Tfb1/p62 is significantly enhanced by diphosphorylation of p53 at both Ser[46] and Thr[55] and that the enhanced binding of each phosphorylation was additive.[49] Mutational analysis in combination with the structure of the Tfb1/p53 complex indicated that the increase in binding due to phosphorylation of Ser[46] is the result of an ionic interaction with Lys[11] of Tfb1, whereas the increase in binding due to phosphorylation of Thr[55] is the result of an ionic interaction with Arg[61] of Tfb1.[49] Thr[55] of p53 aligns with Thr[480] in VP16 so this residue is conserved between p53 and VP16 (Figure 4A). In contrast, Ser[46] of p53 aligns with Ala[471] of VP16C, thus the interaction between phosphorylated Ser[46] of p53 and Lys[11] of Tfb1 does not appear to be conserved in the Tfb1/VP16 complex (Figure 4A). Interestingly, Asp[472] is the residue adjacent to Ala[471] in VP16C, and in a subset of our NMR structures of the Tfb1/VP16C complex it appears that this Asp[472] could form an ionic interaction with Lys[11]. Therefore, this interaction would be somewhat analogous to the interaction observed with the phosphorylated Ser[46] in p53. To determine if an ionic interaction between Lys[11] of Tfb1 and Asp[472] of VP16C is contributing to the binding of VP16C to Tfb1, we mutated Asp[472] of VP16C to alanine [VP16C(D472A)] and we mutated Lys[11] of Tfb1 to glutamic acid [Tfb1(K11E)]. ITC experiments of Tfb1 with VP16C(D472A) demonstrated that Asp[472] is important for the formation of the Tfb1/VP16C complex as this mutant decreased binding by a factor of ∼ 5 when compared to the wild-type VP16C (Table 1). Surprisingly, ITC experiments with VP16C and the Tfb1(K11E) mutant demonstrated that Tfb1(K11E) actually had a slightly higher affinity for VP16C then wild-type Tfb1(Table 1). These results indicate that Lys[11] of Tfb1 does not make a significant contribution to VP16C binding and that there is no apparent ionic interaction between Asp[472] of VP16C and Lys[11] of Tfb1. The role of the negatively charged Asp[472] in the first position of the helix of VP16C in the Tfb1/VP16C complex may be for the stabilization of the α-helix through interaction with the helix dipole.[67,68] This is supported by experiments with model peptides that have shown that aspartic acid at the first position of a helix stabilizes the helix.[69,70]

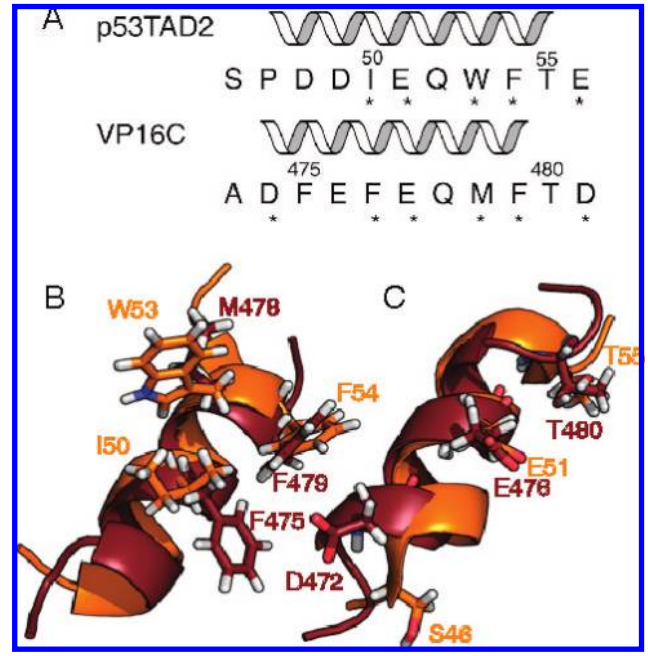

Figure 4. Comparison of VP16C and p53TAD2 in complex with Tfb1. (A) Sequences of human p53TAD2 and Herpes Simplex Virus VP16C are aligned based on the 9-residue α helix with residue numbering and secondary structure elements represented above each protein sequences. An asterisk below a residue indicates that the amino acids show intermolecular NOE(s) with Tfb1 in its respective complex. (B−C) Overlay of residues 45−57 of the p53TAD2 (in orange) and residues 469−482 of VP16C (in red). (B) The three hydrophobic residues from the helix of VP16C (Phe[475], Phe[479] and Met[478]) at the complex interface are aligned with the three hydrophobic amino acids from the helix of p53TAD2 (Ile[50], Phe[54] and Trp[53]) at the complex interface. (C) Glu[476] and Thr[480] of VP16C and Glu[51] and Thr[55] of p53 are in similar positions in the two structures. In contrast, Asp[472] of VP16C and Ser[46] of p53TAD2 are positioned on different faces of the helices.

Comparison of the Structures of the Tfb1/VP16C and Tfb1/p53 TAD2 Complexes. The TADs of VP16 and p53 share several common binding partners, and the residues of p53 TAD2 that form the Tfb1 interface display sequence homology with VP16C (Figure 4A). Thus, one would anticipate that the Tfb1/p53TAD2 and Tfb1/VP16C complexes would display many common features, and this is in fact the case. First, the structure of the PH domain of Tfb1 is essentially unchanged in the two complexes. In addition, one observes the formation of a 9-residue α-helix in the TAD of both p53 and VP16C upon complex formation with Tfb1. The VP16C and p53TAD2 helices both possess a face that contains three hydrophobic amino acid residues that are essential for binding to Tfb1. Superposition of the hydrophobic residues from p53TAD2 and VP16C, clearly demonstrates that they are located in similar positions on the α helices in the two complexes (Figure 4B). The hydrophobic residues also formed similar types of interactions with Tfb1 in the two complexes even though these residues

(67) Wada, A. *Adv. Biophys.* **1976**, *9*, 1–63.
(68) Hol, W. G. L.; Duijnen, P. T. v.; Berendsen, H. J. C. *Nature* **1978**, *273*, 443–446.
(69) Huyghues-Despointes, B. M. P.; Scholtz, J. M.; Baldwin, R. L. *Protein Sci.* **1993**, *2* (10), 1604–1611.
(70) Scholtz, J. M.; Qian, H.; Robbins, V. H.; Baldwin, R. L. *Biochemistry* **1993**, *32* (37), 9668–9676.

are not strictly conserved. VP16C is clearly mimicking p53TAD2 in making several types of contacts with Tfb1 such as hydrophobic, amino−aromatic, cation−π interactions and sulfur−π interactions (Figure 4B). In addition, the ionic interaction involving Glu^{476} of VP16C with Arg^{61} of Tfb1 in the Tfb1/VP16 complex directly mimics the interaction between Glu^{51} of p53 and Arg^{61} of Tfb1 (Figure 4C). Despite the similarities between the Tfb1/p53 and Tfb1/VP16C complexes, there are some important differences that occur at the amino-terminal end of the helices. In the case of p53, there is a proline residue in the first position of the helix (Pro^{47}) that is preceded by a serine residue (Ser^{46}). Ser^{46} of p53 has been shown to be phosphorylated in vivo by the p38 mitogen activated protein kinase (MAPK) and the homeodomain interacting protein kinase (HIPK),[71] and we have previously demonstrated that phosphorylation of Ser^{46} increases the binding affinity of p53TAD2 to Tfb1/p62 *in vitro*. In VP16C, there is an aspartic acid residue in the first position of the helix (Asp^{472}). Our initial assumption was that Asp^{472} of VP16 was serving a similar function as the phosphorylated Ser^{46} in p53. However, mutational analysis clearly demonstrated this is not the case. In addition, it is clear that Ser^{46} of p53 and Asp^{472} of VP16 are oriented very differently with respect to each other (Figure 4C). The different orientations would preclude them from participating in similar interactions with Tfb1. As we proposed earlier, Asp^{472} may stabilize the VP16 helix through interactions with the helix dipole and thereby stabilize its complex with Tfb1. In contrast, the phosphorylated Ser^{46} of p53 forms an ionic interaction with Tfb1/p62 that is dependent on a signaling pathway involving either MAPK or HIPK.[71]

Discussion

In this manuscript, we have examined the interaction of the Tfb1 subunit of TFIIH with the TAD of VP16 at the atomic level. We demonstrate that the VP16C subdomain within the VP16TAD binds with higher affinity to the PH domain of Tfb1 then does VP16N. NMR structural studies demonstrate that VP16C is disordered in the free state, and forms a 9-residue α-helix involving residues Asp^{472} to Thr^{480} in complex with Tfb1. The high-resolution structure of the Tfb1/VP16C complex demonstrates that the VP16C helix contains three hydrophobic residues (Phe^{475}, Met^{478} and Phe^{479}) that make several crucial contacts with Tfb1 via cation−π, sulfur−π, amino−aromatic and hydrophobic interactions. In addition, two acidic residues (Asp^{472} and Glu^{476}) in the VP16C helix also contribute significantly to the stability of the complex. Glu^{476} of VP16C forms an ionic interaction with Arg^{61} of Tfb1, whereas Asp^{472} likely stabilizes the helix dipole of VP16C. The structure and interactions of the VP16C helix in the Tfb1/VP16C complex are remarkably similar to what we previously observed for the 9-residue helix of p53 in our NMR structure of a Tfb1/p53TAD2 complex. It is clear that VP16 mimics p53 in many interactions with Tfb1.[49] Despite the remarkable similarities between the Tfb1/p53TAD2 complex and the Tfb1/VP16C complex, there are some important differences. The differences between the two complexes are at the amino-terminal end of the respective α-helices in VP16C and p53TAD2. For p53, phosphorylation of Ser^{46} significantly enhances binding of the p53TAD2 to Tfb1/p62 through formation of an ionic interaction with Lys^{11} in a loop between β1 and β2 of the PH domain of Tfb1. In the case of VP16, there is no equivalent phosphorylation site present in the sequence, and the closest acidic residue in VP16C (Asp^{472}) that could mimic the phosphoserine of p53 does not interact with Lys^{11} of Tfb1.

The Tfb1/VP16C structure supports many of the previous mutagenesis studies examining the role of VP16C in VP16-dependent activation.[8,24,31,33,54,63,72] These studies demonstrated that mutating the three hydrophobic residues (Phe^{475}, Met^{478} and Phe^{479}) in the VP16C helix to proline almost completely eliminates VP16 activation of target genes but that mutation of these residues to alanine or other hydrophobic residues such as leucine has a significanltly less dramatic effect on activity. Based on the Tfb1/VP16 complex structure, it is evident that mutation of these three hydrophobic residues to proline should significantly alter the interaction of VP16 with Tfb1 by disrupting formation of the α-helix, and the results from our ITC experiments confirm this. In addition, the F475A and F479A mutants decrease the binding of VP16C to Tfb1 by only 2.8-fold and 2.5-fold respectively and the decrease in binding observed with these two mutations is consistent with the fact that these mutants retain 25% of their activity in vivo.[72] It is also similar to what has been previously observed with TBP where the F475A mutant decreased VP16C binding to TBP by 2.3-fold and the F479A mutant decreased VP16C binding to TBP by 2.7-fold.[72] Given the fact that alanine is a common amino acid in α helices, it appears that the F475A and F479A mutants do not disrupt formation of the helix in VP16C and this leads to a much smaller effect on VP16C binding to Tfb1 and transcriptional activity then the proline mutants. In comparing VP16C/Tfb1 complex with the p53TAD2/Tfb1 complex, Phe^{475} of VP16C occupies the same position in the helix as Ile^{50} of p53. Phe^{475} forms a cation-π interaction with Arg^{61} and a sulfur-π interaction with Met^{88} on Tfb1 (Figure 3B) and Ile^{50} forms van der Waals interactions with Met^{59} and Met^{88} of Tfb1.[49] In the case of VP16C (F475A), the methyl group of alanine could position itself in a similar manner as one of the methyl groups of Ile^{50} and participate in van der Waals interactions with Tfb1. This would partially compensate for the interactions lost with the aromatic ring of Phe^{475} and this would explain why only a small decrease in binding is observed with the VP16C (F475A) mutant. A similar argument could be used to explain why the F475L mutant of VP16C has similar activity as wild-type VP16C *in vivo*.[72] Likewise, Phe^{479} occupies the same position in the helix as Phe^{54} of p53. These two residues are identical and their side chain fills a shallow pocket formed by Gln^{49}, Ala^{50}, Thr^{51}, $Met,^{59}$ Leu^{60} and Arg^{61} of Tfb1. Specifically, the aromatic ring participates in cation-π interactions with Arg^{61} and amino-aromatic interactions with Gln^{49} of Tfb1 in both complexes. It is clear that the alanine mutant cannot participate in similar interactions with Tfb1 but it could participate in van der Waals interactions with Ala^{50}, Thr^{51}, Met^{59} or Leu^{60} of Tfb1. The van der Waals interactions would partially compensate for the interactions observed with the aromatic ring. Again as suggested for Phe^{475}, a series of van der Waals interactions would explain why the VP16C (F479L) mutant has similar activity to the wild-type VP16C.[72]

The structure of the Tfb1/VP16 structure also indicates that Phe^{473} within VP16C does not play a critical role in the formation of the interface with Tfb1 (Figure 3A). Mutagenesis studies indicate that although Phe^{473} is important for transcriptional activation by VP16C, equivalent substitutions at Phe^{475}

(71) Bode, A. M.; Dong, Z. *Nature Rev. Cancer* **2004**, *4* (10), 793–805.

(72) Nedialkov, Y. A.; Shooltz, D. D.; Triezenberg, S. J. *Methods Enzymol.* **2003**, *370* (RNA Polymerases and Associated Factors, Part C), 522–535.

and Phe[479] have more pronounced effects.[24,63] Based on the structure of the Tfb1/VP16 complex, it appears that Phe[473] plays a secondary role by stabilizing the formation of the helix or that it is important for other interactions during the transcription process. This is supported by the fact that mutation of Phe[473] to proline completely abolishes transcriptional activity whereas mutation of Phe[473] to alanine has very little effect.[72] These results are consistent with the fact that the proline mutation would block formation of the helix and the alanine mutation would allow for formation of the helix.

In addition to hydrophobic residues, mutational analysis indicates that acidic residues are important for VP16C-dependent activation albeit less critical then hydrophobic residues.[22,24,63] The structure of the complex indicates that many of the acidic residues of VP16C probably play a more general role by contributing to binding through a nonspecific electrostatic effect with the basic binding site on Tfb1. This is consistent with mutagenesis studies indicating that for several cases multiple acidic residues must be mutated before one observes a decrease in VP16C-dependent activation.[22] Our structure of the complex does demonstrate that there is one crucial ionic interaction involving Glu[476] of VP16C and this is consistent with the fact that mutation of Glu[476] to alanine results in a 55% decrease in VP16C activity in a yeast-based transcriptional activation assay.[63] The role of Asp[472] is more complex. Our results indicate that Asp[472] of VP16C plays a crucial role in binding to Tfb1 although no direct ionic interaction is formed. In our NMR studies, we observe significant chemical shift changes in Asp[472] indicating that it is near the interface in the VP16C/Tfb1 complex. Similar chemical shift changes for Asp[472] have been observed in previous NMR studies examining VP16C binding to TFIIB, PC4 and human$TAF_{II}31$.[31,33] In addition, our ITC studies clearly demonstrate that alanine substitution at Asp[472] significantly reduces VP16C binding to Tfb1. We attribute this to the fact that Asp[472] is stabilizing the formation of the helix through interactions with the dipole moment. However, previous studies indicate that the D472A mutation does not alter the transactivation capacity of VP16C.[24] There are several possible explanations for this observation including the possibility that the D472A mutation is having a stabilizing effect on VP16C turnover and this helps compensate for the loss in binding activity. However, additional studies are required to understand more clearly the role of Asp[472] in VP16C binding to Tfb1.

It is interesting to compare our Tfb1/VP16C NMR structure with the results of other NMR studies examining the interactions of the VP16TAD with partner proteins. Two other studies have used NMR spectroscopy to examine the interactions of the VP16TAD with target proteins.[31,33] The first study examined binding between VP16C and $TAF_{II}31$.[31] This study predicted that a 12-residue helix formed between Asp[472] and Leu[483] in VP16C when in complex with $TAF_{II}31$. The second study[33] examined interactions between the full VP16TAD and TFIIB and PC4. In the second study, a 21-residue helix was predicted to form between Pro[465] and Ile[485] of VP16C when in complex with either TFIIB or PC4. As was seen in our Tfb1/VP16C complex, each of these studies provided strong NMR experimental evidence for the formation of an α-helix in VP16C upon complex formation with the partner proteins. In both studies, the residues predicted to form the helix overlap with the VP16C residues that interact with Tfb1 in our Tfb1/VP16C complex. Consistent with our results, mutational analysis of VP16C indicated that Phe[479] was extremely crucial for the interaction with $TAF_{II}31$, TFIIB and PC4.[31,33] The difference between our results and results from previous studies is that the helix in the Tfb1/VP16C complex is slightly shorter then the helices from the three other complexes. Together, this suggests that VP16C might use similar interactions when binding to $TAF_{II}31$, TFIIB and PC4 and that a binding pocket for Phe[479] is clearly a crucial determinant for interaction with VP16C.

The comparison of the Tfb1/p53 and Tfb1/VP16 structures is an important step toward developing a better understanding for acidic TADs binding to target proteins and in particular acidic TADs binding to the Tfb1/p62 subunit of TFIIH. Such detailed structural information is absolutely essential to our efforts to design molecules that mimic transcription activators such as p53 and VP16. For example, it is now clear that the VP16C interacting helix aligns much better with the p53TAD2 helix as opposed to p53TAD1 helix as earlier reports suggested.[31,32] Based on the structures of the two Tfb1 complexes, it is now possible to develop several simple rules that would begin to describe the requirements for a 9-residue helix binding to Tfb1/p62 subunit of TFIIH. The rules would start with position 3 through 9 in the α-helix and these 7 positions make a significant number of interactions found at the complex interface. The simplified sequence for position 3 through 9 would be D/EΦEQΦΦT, where Φ is a hydrophobic residue with a slight preference for phenylalanine. Although the glutamine at position 6 is conserved between VP16 and p53, it does not contribute significantly to the interaction surface. Therefore this residue may not be strictly conserved in other acidic TADs that bind to p62/Tfb1. The threonine at position 9 (Thr[55] in p53 and Thr[480] in VP16C) does not contribute significantly to binding in the case of p53 unless it is phosphorylated. To date there is no evidence that Thr[480] of VP16 is phosphorylated, but it would be in position to make similar contributions as the phosphorylated Thr[55] does in the p53/p62 and p53/Tfb1 complexes (Figure 4C). The requirements for the first two positions of the helix are not well defined by the two structures. Not surprisingly, the Tfb1/p62 subunit has been shown to interact with a number of additional transcriptional activators that contain acidic TADs, including the p65 subunit of NFκB,[73] E2F1,[74] EBNA2[75,76] and CIITA.[77] In each case, the TAD within the proteins contains a number of hydrophobic amino acids in addition to being highly acidic and therefore these domains are likely binding sites for p62/Tfb1. Structures of Tfb1/p62 in complex with other acidic TADs are needed to better define the requirements for the nine-residue helix.

The structure of the Tfb1/VP16C complex is the first high-resolution structure of the TAD of VP16 in a protein/protein complex. The structure sheds light on the role of the general transcription machinery in VP16 transcriptional activation. The structure of the Tfb1/VP16C complex in combination with our previous NMR structure of the Tfb1/p53 complex[49] enables us to make a detailed comparison between a mammalian activator (p53) and a viral activator (VP16) on a common member of the general transcription machinery (Tfb1). Our results clearly demonstrate how the viral activator VP16 is very similar to the mammalian activator p53 when in complex with Tfb1. In

(73) Kim, Y. K.; Bourgeois, C. F.; Pearson, R.; Tyagi, M.; West, M. J.; Wong, J.; Wu, S.-Y.; Chiang, C.-M.; Karn, J. *EMBO J.* **2006**, *25* (15), 3596–3604.
(74) Pearson, A.; Greenblatt, J. *Oncogene* **1997**, *15*, 2643–2658.
(75) Wang, B. Q.; Burton, Z. F. *J. Biol. Chem.* **1995**, *270*, 27035–27044.
(76) Tong, X.; Wang, F.; Thut, C. J.; Kieff, E. *J. Virol.* **1995**, *69* (1), 585–588.
(77) Mahanta, S. K.; Scholl, T.; Yang, F.-C.; Strominger, J. L. *Proc. Natl. Acad. Sci. U.S.A.* **1997**, *94* (12), 6324–6329.

addition, the structures of the Tfb1/VP16 and Tfb1/p53 complexes demonstrate how simple changes in the sequence could alter the requirement for post-translational events such as phosphorylation. It is interesting to point out that most of the acidic TADs studied to date are intrinsically unstructured in the free state, but form α-helices in complex with their target proteins as is seen with p53 and VP16 in complex with Tfb1.[31,33,41–43,49,78] This observation, in combination with the fact that phosphorylation events often take place in unstructured regions of proteins,[79] suggests that phosphorylation events within acidic TADs can play an important role in regulating their interactions with partner proteins. Future structural studies with other mammalian and viral activators bound to Tfb1/p62 are needed to better understand this form of regulation in the case of TFIIH. In addition, more detailed structure−function studies are needed to further refine the precise requirements for acidic TADs binding to Tfb1/p62 and other target proteins.

Coordinates. The atomic coordinates of the Tfb1/VP16C complex have been deposited in the Protein Data Bank, www.rcsb.org (2k2u).

Acknowledgment. We thank Jimmy Dikeakos for critical reading of this manuscript. We thank Steven Triezenberg for providing the GST-VP16C and GST-VP16N clones. This work was supported by NCIC grant 016302 with funds from the Terry Fox Foundation, (J.G.O.). C.L. is recipient of a Postdoctoral Fellowship from the FQRS. P.D.L is recipient of a Postdoctoral Fellowship from the CIHR. P.L. is a Canadian research chair in structural biology of RNA.

Supporting Information Available: Supplementary Figure 1 shows the full ITC curve for the binding of VP16C to Tfb1. Supplementary Figure 2 shows those residues of $Tfb1_{1-115}$ that undergo significant chemical shift changes in 2D $^{1}H-^{15}N$ spectra upon addition of 1 equivalent of VP16C. Supplementary Figure 3 shows a superposition of 2D $^{1}H-^{15}N$ spectra of ^{15}N-labeled VP16C free and after addition of varying amounts of $Tfb1_{1-115}$. Complete ref 15. This material is available free of charge via the Internet at http://pubs.acs.org.

JA800975H

(78) Dahlman-Wright, K.; Baumann, H.; McEwan, I. J.; Almlof, T.; Wright, A. P.; Gustafsson, J. A.; Hard, T. *Proc. Natl. Acad. Sci. U.S.A.* **1995**, *92*, 1699–1703.

(79) Iakoucheva, L. M.; Radivojac, P.; Brown, C. J.; O'Connor, T. R.; Sikes, J. G.; Obradovic, Z.; Dunker, A. K. *Nucleic Acids Res.* **2004**, *32* (3), 1037–1049.